Stability of coarse bed material in open channels

Atef Abdel-Hameed El-Saiad
Water and Water Structures Eng. Dept., Faculty of Eng., Zagazig University, Zagazig, Egypt

The present paper deals with the effect of flow parameters on the stability of non-uniform rough bed materials. The stability of rough bed material is studied experimentally by using two samples of crushed limestone of mean diameter 0.48cm and 0.82cm respectively. Experiments were carried out in tilting steel recirculating flume with glass side walls. For the two tested samples the critical shear stress is determined when the bed particles just begin to move (in vibration state or weak movement state). The relation between main factors affecting the incipient motion such as the flow parameters and the bed material characteristics are studied experimentally. Empirical equations for calculating the critical shear stress at the incipient motion condition and the friction factor coefficient are developed by using the statistical analysis methods.

هذه الدراسة تتناول دراسة تأثير متغيرات السريان المختلفة على أتزان حبيبات القاع الخشنة و الغير منتظمة التدريج. وقد تمت الدراسة المعملية فى قناة معملية مستطيلة الشكل ذات جوانب زجاجية وذلك بدراسة أتزان عينة من الحجر الجيرى المتدرج بقاع القناة ذات قطر متوسط ٠,٤٨ سم و٠,٨٢ سم كل على حدة وتم قياس متغيرات السريان المختلفة لجميع التجارب لعينتى الركام المتدرج فى حالة بداية حدوث حركة ضعيفة واهتزازات لحبيبات القاع وتم حساب القيمة الحرجة لأجهاد القص عند بداية الحركة لحبيبات القاع. وتم دراسة العلاقة بين متغيرات السريان وخصائص مادة القاع كما تم استخدام التحليل القياسى والإحصائي لإيجاد معادلات تجريبية لحساب قوى السريان الحرجة المسببة لبداية حدوث حركة لحبيبات الحجر الجيرى بقاع القناة وكذلك تم استنباط معادلات تجريبية أخرى لحساب قوى القص الحرجة على حبيبات القاع عند بداية حدوث الحركة ومعامل الخشونة لحبيبات القاع.

Keywords: Critical shear stress, Incipient motion, Friction factor, Bed shear velocity

1. Introduction

The critical shear stress affecting the stability of bed material and the friction coefficient are studied in this paper. The bed particles remain stable when the shear stress is less than the critical value of shear stress. When the critical shear stress over the bed attains or exceeds its critical value, the bed particles starts to move. Sediment entrainment is defined as the transition from repose to displacement. The critical shear stress and the friction coefficient for coarse bed material still needs more studies. The scope of this study is to analyze and presents statistical models for estimating the critical shear stress and the friction coefficient of coarse bed material in open channels. The models are calibrated and checked using the collected experimental data and good agreement is existed.

Several researchers have studied the effect of flow forces on the stability of different bed material. Halow [1] Darke et al. [2] indicated that the entrainment of sediment particles occurs in different ways, namely, rolling, sliding, lifting and bouncing (or impact ejection). The initiation of particle motion by sliding or bouncing occurs only rarely and is much less important than the other two modes, thus often neglected in the analysis. Shields diagram is widely used for uniform sediments. However the high degree of scatter in the experimental data has resulted in attempts to revise the diagram. A few alternative to the Shields threshold curve have been proposed giving fairly wide range of threshold flow conditions (Miller et al. [3], and Misri et al. [4]). Gessler [5] determined from their data sets that the critical Shields parameter (τ_*) for sediment mixtures was about 0.047. Neill [6] concluded that in gravel mixtures, most of particles become mobile when the critical Shields parameter (τ_*) for median grain size was 0.030. One of the most obvious reasons for the systematic differences between various studies is the subjectively identifying the threshold of sediment motion Miller et al. [3]. Yalin and Karahan [7] studied the inception of sediment transport and

© Faculty of Engineering Alexandria University, Egypt.

derived the relation between the non dimensional critical bed shear stress and the corresponding particles Reynolds number. Andrews [8] found a slight difference in τ_*, for different grain sizes in mixture. He found that the minimum value of τ_* is equal to 0.020. Ling [9] further derived the rolling and lifting criteria for incipient motion of spherical sediment particles. His results revealed that the lifting threshold is consistently higher than the rolling threshold in hydraulically smooth and transitional flow regimes. Dey and Raju, [10] studied the incipient motion of gravel and coal beds. They derived an empirical equation for estimating the critical bed shear stresses for the incipient motion of gravel.

Estimation of flow resistance in open channel flows is essential. Traditionally flow resistance is predicted by means of Manning and Darcy-Weisbach equations. These equations were developed for uniform and steady flow. Several researchers have proposed different equations to estimate Darcy-Wesbach friction coefficient for rough bed material in open channels. Bathurst [11], French [12], Graf [13], Rice et al. [14] studied the friction coefficient in open channels for hydraulically smooth and rough bed material. They derived different equations for estimating the Darcy-Wesbach friction factor as a function of relative submergence ratio of particle size and hydraulic radius. The derived equations are different according to the friction slopes. The main purpose of this study is to analyze the experimental data and present statistical model for estimating the critical shear stress and the friction coefficient of coarse bed material.

2. Dimensional analysis

In general it is possible to state that the threshold condition for the beginning of particle motion depends on: τ_c, d, D_{50}, g, ρ_S, ρ, R_b, ν, U_{*b}, U_*, U. A dimensional analysis yields the following relationship,

$$\frac{\tau_c}{(\gamma_S-\gamma)D_{50}} = f\left(\frac{D_{50}}{R_b}, \frac{D_{50}}{d}\, \frac{\rho_S}{\rho}, \frac{U_{*b}}{U}\, R_{e*b}, F_{rb}\right),$$

in which,

D_{50} is the mean diameter of grains,
d is the water depth,
F_{rb} is the grain Froude number ($F_{rb} = U/\sqrt{gR_b(S_G-1)}$,
R_b is the hydraulic radius of bed,
R_{e*d} is the bed Reynolds number U_*D_{50}/ν,
U is the mean velocity,
U_* is the shear velocity at threshold condition,
U_{*b} is the bed shear velocity at threshold condition,
ρ is the mass density of water,
ρ_S is the mass density of sediment,
γ is the specific weight of water,
γ_S is the specific weight of sediment,
ν is the kinematic viscosity of water, and
τ_C is the critical shear stress.

2.1. The bed friction factor (f_b)

Vanoni's [15] method of side wall correction factor for rectangular flume is used here. Thus the Chezy equation can be written in the following form:

$$\frac{U^2}{S} = \frac{8gR}{f} = \frac{8gR_b}{f_b} = \frac{8gR_w}{f_w}, \tag{1}$$

in which; R= the hydraulic radius, S = the energy slope, and f = the total friction factor coefficient of section. The subscript (w) and (b) refer to the side walls and the bed respectively,
Then,

$$\frac{A}{Pf} = \frac{A_b}{f_bP_b} = \frac{A_w}{f_wP_w}, \tag{2}$$

in which, A= cross sectional area, and P= wetted perimeter.

From the continuity equation the discharge (Q) can be expressed,

$$Q = AV = A_wU_w + A_bU_b. \tag{3}$$

The mean velocity is the same for the bed and the walls

$$A = A_w + A_b. \tag{4}$$

By substituting from eq. (2) in eq. (4) then,

$$f_b = \frac{Pf}{P_b} - \frac{P_w f_w}{P_b}. \tag{5}$$

The wetted perimeter of the rectangular section $P = 2d + b$, the wetted perimeter of the two side walls $P_w = 2d$, and the wetted perimeter of the bed (P_b) = bed width (b).

By substituting with the above values in eq. (5) then,

$$f_b = f + \frac{2d}{b}(f - f_w), \tag{6}$$

$$\therefore f_w = \frac{8g \times n_w^2}{R_w^{1/3}}. \tag{7}$$

Assume, the Manning roughness coefficient for glass walls of flume = n_w = 0.009, then f_w can be obtained from eq. (7) and the friction factor coefficient (f_b) can be calculated from eq. (6). The critical bed shear stress can be obtained from the following equation,

$$\tau_{cb} = \gamma \times R_b \times S. \tag{8}$$

3. Experimental study

The experimental study was carried out in a 0.45m deep, 0.30m wide, and 12.50m long re-circulating flume with vertical glass sides and an Aluminium bed, in the hydraulic laboratory, Zagazig University, Egypt, during the year (2002). A sample of a crushed limestone of specific gravity 2.65 and angle of repose of 39^o was used as rough bed material. The sizes of the two tested samples are ranged between 3.35mm and 6.30mm for the first sample, and 6.30mm to 10.0mm for the second sample. The mean diameter of the two tested samples is D_{50}= 0.48cm and 0.82cm, with equivalent roughness height k_s= D_{65} = 0.52cm and 0.86cm respectively (Patal & Ranja Raju [16]. The geometric standard deviation for the two tested samples is equal to $\sigma = (D_{84}/D_{16})^{0.5}$ = 1.22 and 1.17 respectively. The stone blanket thickness = $4D_{50}$ and 4.0 m length. Under the tested sample, a cloth filter was placed over sand layer of 8cm thickness. The sides of the flume in the test section were made of glass enabling observation of the movement of bed particles. At the beginning of each run the bed material was leveled. The downstream control gate is closed initially. Water was passed gradually through the working section by gradually opening the upstream valve. After the bed was completely submerged, the downstream gate was opened gradually. At the same time the upstream discharge was adjusted so that the incipient motion condition was reached when some of bed particles on the surface start in vibration and rolling. When the incipient motion of bed particles occurs, the discharge (Q), and the corresponding water depth y were recorded. The flow depth (d) is measured from the free water surface to the virtual bed level. The virtual bed level was considered to be at $0.25D_{50}$ below the top level of the bed particles (Dey [17]). Fig. 1 shows the definition sketch of the tested model.

5. Analysis and discussions

For the two tested samples, the values of dimensionless shear stress $\tau_* = \tau_c/(\gamma_s - \gamma)D_{50}$ is plotted against grain Reynolds number ($R_{e^*d} = U_* D_{50}/\nu$) in fig. 2. The incipient motion data that obtained by Dey and Raju

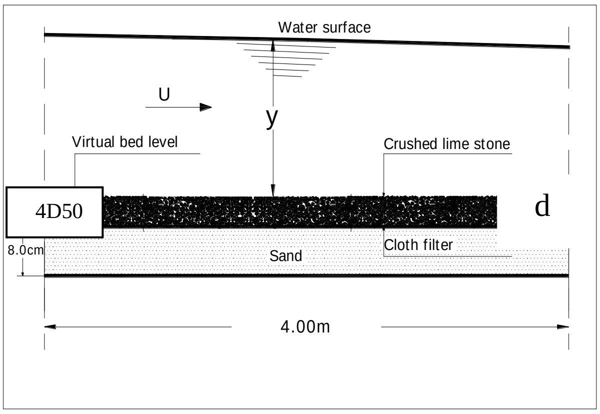

Fig. 1. Definition sketch.

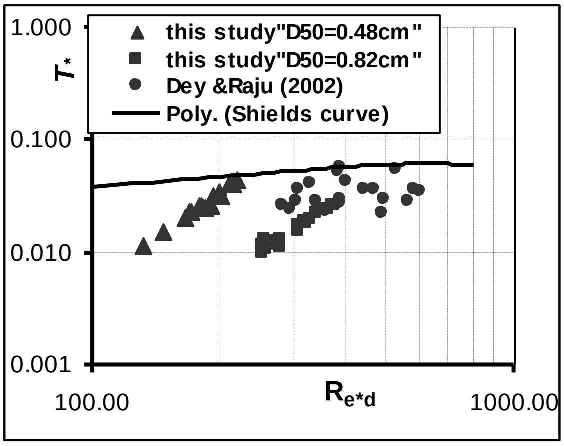

Fig. 2.Comparison between shields diagram and the present study.

[14], are also shown on the same figure. This figure shows that, the dimensionless shear stress increases by increasing the particle Reynolds number within the range ($0.01 \le \tau_* \le 0.046$ and $165 \le R_{e*d} \le 380$). The experimental data plotted on this figure show that, the dimensionless shear stress values are in good agreement with that obtained by Dey and Raju [10] and less than standard Shields diagram (which was plotted for uniform bed material). This decreasing trend in (τ_*) values due to the difference in particle size and shape furthermore the incipient motion in this study taken at vibration case which leads to roll few particles. The relation between the critical values of dimensionless bed shear stress ($\tau_{*b} = \tau_{cb}/(\gamma_s - \gamma)D_{50}$) is plotted against shear Reynolds number of bed ($R_{e*b} = U_{*b}R_b/\upsilon$) in fig. 3. This figure shows that the dimensionless bed shear stress increases by increasing the shear Reynolds number of bed. Also, the values of (τ_{*b}) decreases by increasing the mean diameter for the same shear Reynolds number value. Fig. 4 shows the variation of dimensionless bed shear stress (τ_{*b}) and the relative particle size (D_{50}/R_b). This figure indicates that the dimensionless shear stress (τ_{*b}) decreases by increasing the relative roughness (D_{50}/R_b). This means that the dimensionless shear stress is affected by the relative roughness height in addition to the hydraulic radius of bed according to the following equation,

$$\tau_{*b} = 0.0008 \times (D_{50}/R_b)^{-1.19}, \quad \text{for} \quad (0.05 \le D_{50}/R_b \le 0.17). \tag{9}$$

Eq. (9) has a determination coefficient, R^2= 0.85. The relation between critical bed shear stress (τ_{cb}) and the grain Froude number ($F_{rb} = U/\sqrt{gR_b(S_G - 1)}$) have been plotted in fig. 5. This figure shows that the critical bed shear stress decreases by increasing the grain Froude number according to the following equation,

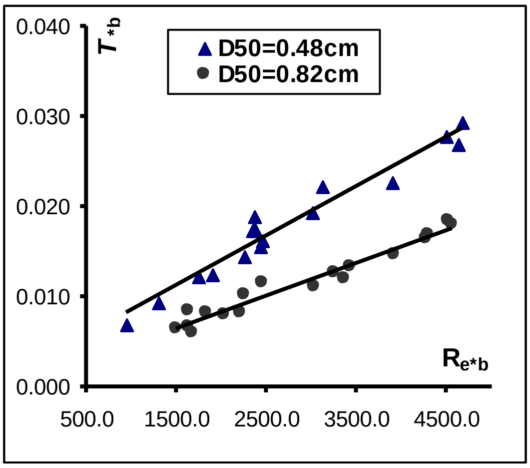

Fig. 3.The relation between T*b and Re*b.

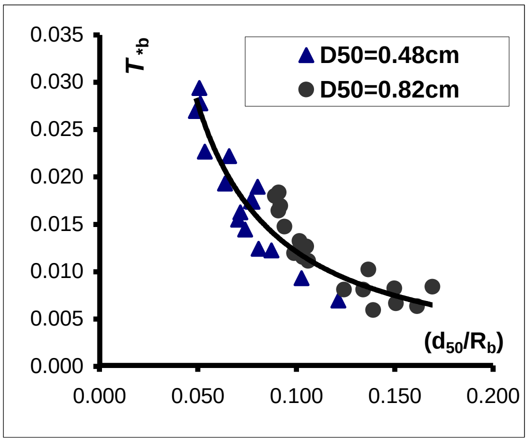

Fig. 4. The relation between T*b and d50/Rb.

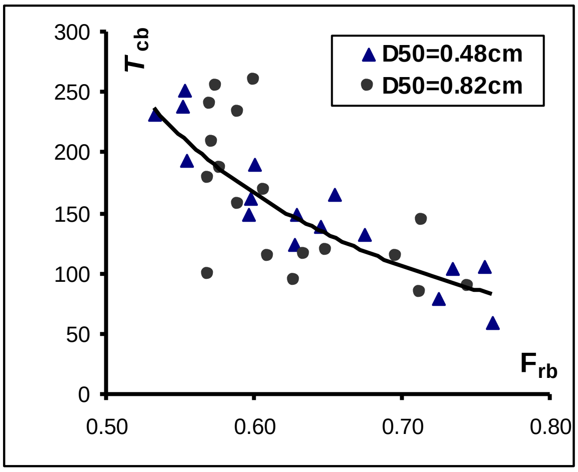

Fig. 5. The relation between Tcb and Frb.

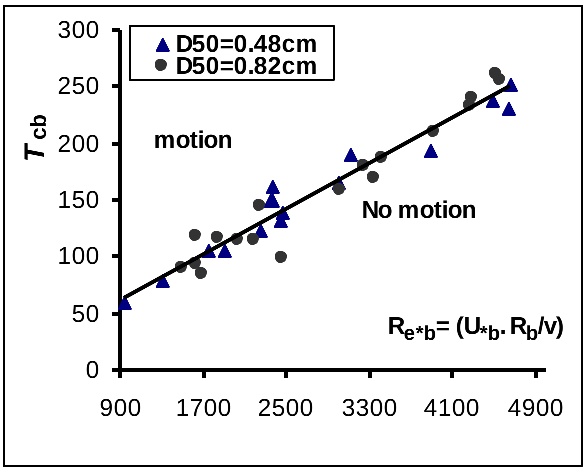

Fig. 6. The relation between Tcb and Re*b.

$$\tau_{cb}(gm/m^2) = 37.1 \times F_{rb}{}^{-2.94}\ , \quad \text{for} \quad (0.53 \le F_{rb} \le 0.77\ ). \qquad (10)$$

Figs. 3- 5, show that the critical conditions of sediment motion depends not only on the grain size but also on the grain Froude number. Fig. 6 shows the relation between the critical bed shear stress ($\tau_{cb} = \gamma R_b S_e$) and the critical shear Reynolds number of bed $R_{e*b} = U_{*b} R_b / \nu$. This figure shows that the critical bed shear stress increases linearly by increasing the critical Reynolds number of bed according to the following equation,

$$\tau_{cb}(gm/m^2) = 0.05 R_{e*b} + 15.8\ , \quad \text{for} \ (900 \le R_{e*b} \le 4900\ ). \qquad (11)$$

The determination coefficient of eq. (11) is equal to (R^2 =0.95). It can be noted that the line which represent the values of eq. (11) is the separate line between the stability and the incipient motion case of bed material. This means that eq. (11) is suitable for studying the critical shear stress over rough bed material of non-uniform size within the range ($900 \le R_{*eb} \le 4900$). Fig. 7 shows the relation between the critical bed shear stress (τ_{cb}) and the relative bed shear velocity (U_{*b} / U). This figure shows that the critical bed shear stress increases by increasing the relative bed shear velocity. The critical bed shear stress can be obtained from eq. (12) which has determination coefficient R^2=0.88.

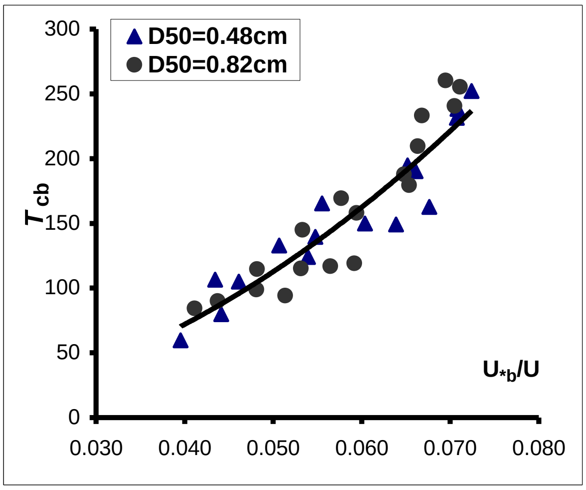

Fig. 7. The relation between Tcb and U*b/U.

$$\tau_{cb}(gm/m^2) = 46017 (U_{*b}/U)^{2.007}, \quad \text{for} \ (0.038 \le U_{*b}/U \le 0.073\ ). \qquad (12)$$

Figs. 8 and 9 show the relation between the measured and the calculated values of (τ_{*b}) and (τ_{cb}) which were obtained using multiple linear regression analysis by using the empirical eqs. (13) and (14) respectively.

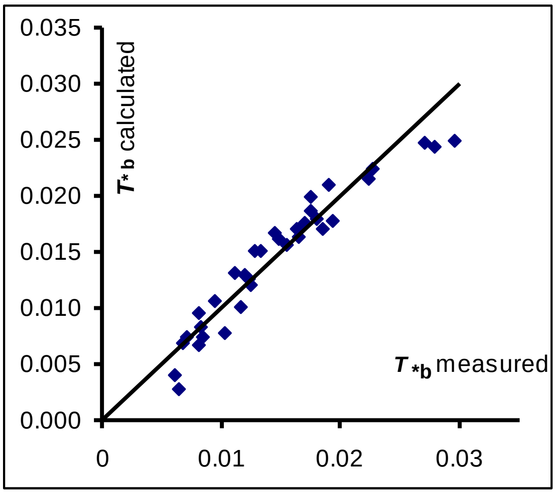

Fig. 8. The relation between the measured and the calculated values of T*b.

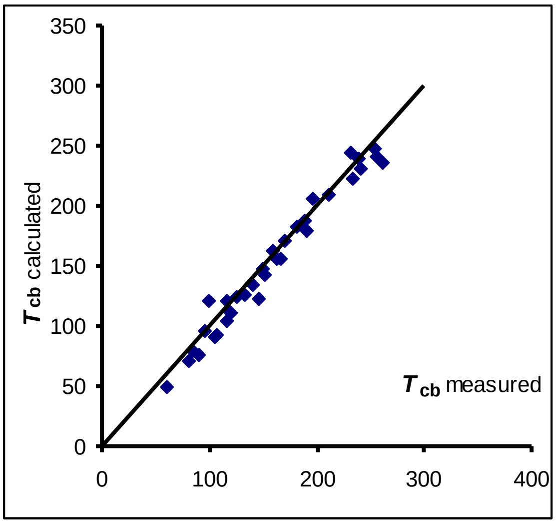

Fig. 9. The relation between the measured and the calculated values of Tcb.

$$\tau_{*b} = 0.0068 - 0.096\frac{D_{50}}{R_b} - 1.90\times10^{-5}\frac{U_* k_s}{\upsilon} + 0.377\frac{U_{*b}}{U}, \qquad (13)$$

$$\tau_{cb}(gm/m^2) = 56.9 - 23.3\frac{D_{50}}{R_b} + 1919\frac{U_{*b}}{U} + 0.036\frac{U_{*b}R_b}{\nu}. \qquad (14)$$

Eq. (13) and (14) have the determination coefficient R^2= 0.96 and 0.99 respectively.

5.1. Friction factor of bed material (f_b).

From the theoretical study the friction factor (f_b) can be calculated from eq. (6). Fig. 10 shows the variation in friction factor coefficient (f_b) versus (U_*/U). This figure shows that the friction factor increases by increasing the relative shear velocity (U_*/U). From this figure the Darcy's friction factor of bed material (f_b) can be obtained by using following equation;

$$f_b = 116.95(U_*/U)^{2.87}$$
for $(0.042 \le U_*/U \le 0.063)$. (15)

The above equation with determination coefficient R^2 = 0.99. Eq. (15) could be used in estimating the bed friction factor (f_b). Fig. 11 shows the relation between the bed friction factor (f_b), and the grain Froude number, $F_{rb} = U/\sqrt{gR_b(S_G-1)}$). This figure shows that the bed friction factor increases by decreasing the grain Froude number due to the increase in the values of hydraulic radius of bed (R_b). Also, fig. 12 shows that the friction factor (f_b), increases by increasing the shear Reynolds number of bed. ($R_{e*b} = U_{*b}R_b/\upsilon$) due to the increase in the values of bed shear velocity (U_{*b}) and hydraulic radius of bed (R_b). fig. 13 shows that the friction coefficient of bed material for hydraulically rough flow ($U_* k_s l\nu \ge 70$) that can be expressed by the following equation,

$$\frac{1}{\sqrt{f_b}} = 10.53 - 4.23\log\frac{R_b}{k_s}$$
for $(5.5 \le R_b/k_s \le 19.0)$. (16)

Eq. (16) is applicable for hydraulically rough flow in open channels.

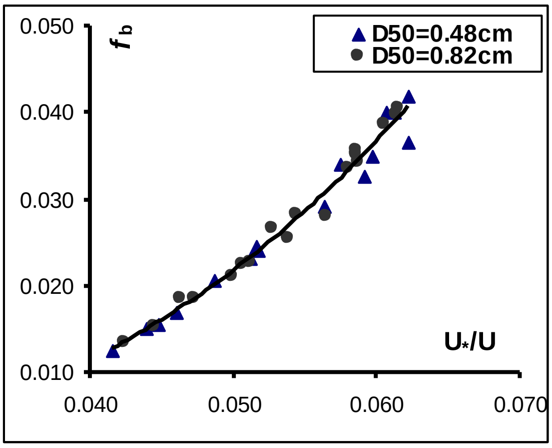

Fig.10.The relation between fb and U/U*.

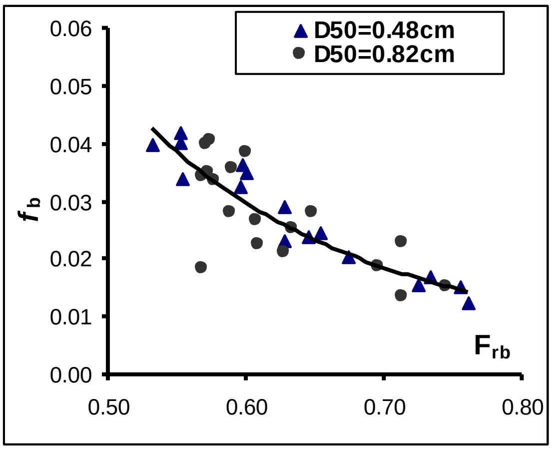

Fig.11. The relation between fb and Frb.

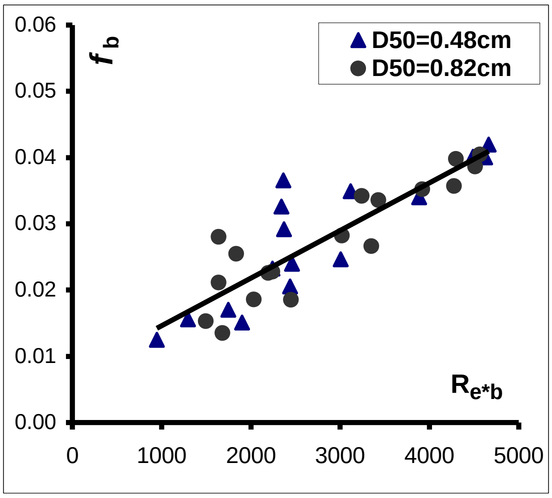

Fig.12.The relation between fb and Re*b.

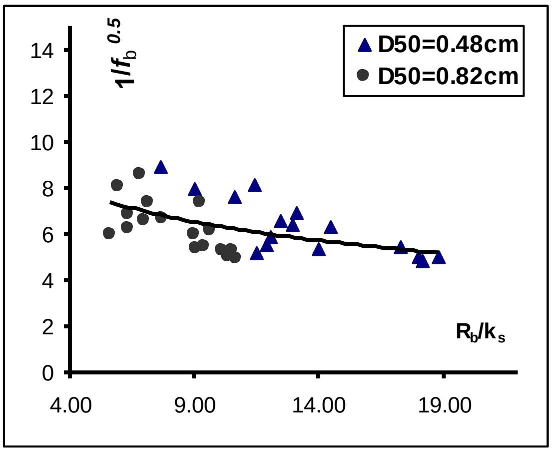

Fig.13.The relation between 1/fb0.5 and Rb/ks.

6. Conclusions

The experimental study is conducted for determining the critical bed shear stress, the dimensionless shear stress at initiation of motion condition and the friction factor coefficient for the coarse bed material. The analysis of the experimental data yields the following conclusions.

• Theoretical models are developed for computing the dimensionless shear stress (τ_{*b}) and the critical shear stress τ_{cb} by using eqs. (13 and 14). The prediction of the model agreed well with the experimental results. The obtained results are used to investigate the effect of the particle size, critical Reynolds number and the relative bed shear velocity on the stability of coarse bed material.

• The friction factor of coarse bed material (f_b) can be calculated by using the developed empirical eqs. (15) and (16) as a function of the relative shear velocity and the ratio of hydraulic radius of bed to the roughness height.

Notations

A	is the cross sectional area,
b	is the channel width,
C	is the chezy's coefficient,
d	is the water depth,
D_{50}	is the mean diameter of grains,
D_{16}	is the particle diameter at percentage passing 16% of total weight of sample,

D_{65} is the particle diameter at percentage passing 65% of total weight of sample,
D_{84} is the particle diameter at percentage passing 84% of total weight of sample,
F_{rb} is the bed froude number,
f is the friction factor,
f_b is the friction factor of bed,
f_w is the friction factor of wall,
g is the gravitational acceleration,
k_s is the roughness height $\cong D_{65}$,
n is the manning roughness coefficient of channel,
n_w is the manning roughness coefficient of wall,
n_b is the manning roughness coefficient of bed,
P is the wetted perimeter of the rectangular section,
P_w is the wetted perimeter of the walls=2d,
P_b is the wetted perimeter of the bed = bed width (b),
Q is the discharge,
R is the hydraulic radius,
R_b is the hydraulic radius of bed,
R_w is the hydraulic radius of wall,
R_{e*d} is the grain Reynolds number $(= U_* D_{50} / \nu)$,
R_{e*b} is the bed Reynolds number $(= U_* R_b / \nu)$,
S is the energy slope,
S_G is the specific gravity of crushed limestone,
U is the mean velocity of flow = Q/A,
U_b is the flow velocity at channel bed,
U_w is the flow velocity at channel walls,
U_* is the shear velocity at threshold condition,
U_{*b} is the bed shear velocity at threshold condition,
ρ is the density of water,
ρ_S is the density of coarse bed material,
ν is the kinematic viscosity of water,
τ_* is the dimensionless shear stress $= \tau_c / (\gamma_s - \gamma) D_{50}$,
τ_{*b} is the critical values of bed shear stress $= \tau_c / (\gamma_s - \gamma) k_s$,
τ_c is the critical shear stress = $\gamma R S$,
τ_{cb} is the critical shear stress over bed material = $\gamma R_b S$,
γ is the specific weight of water,
γ_s is the specific weight of bed material, and
σ is the geometric standard deviation $= (D_{84} / D_{16})^{0.5}$.

References

[1] J.S. Hallow, "Incipient Rolling, Sliding and Suspension of Particles in Horizontal and Inclined Turbulent Flow," Chem. Eng. Sci., Vol. 28, pp. 1-12 (1973).

[2] T.G. Drake, R.L. Shreve, W.E. Dietrich, P.J. Whiting, and L.P. Leopold, "Bed Load Transport of Fine Gravel Observed by Motion-Picture Photography, J. luid Mech., Vol. 192, pp. 193-217 (1988).

[3] M.C. Miller, I.N. McCave, and, P.D. Komer, "Threshold of Sediment Motion Under Unidirectional Currents Sedimentology," Vol. 24. pp. 507-527 (1977).

[4] R.L. Misri, R.J. Garde, and K.G. Ranga Raju, "Experiments on Bed Load Transport of Nonuniform Sand and Gravels, Proceedings of the second International Symposium on River Sedimentation," (11-16 October). Beijing, China, pp. 440-450 (1983).

[5] J. Gessler "Beginning and Ceasing of Sediment Motion, Chapter 7, and Aggradation and Degradation," Chapter 8, River Mechanics, Vol. 1, H.W. Shen, ed. And publisher, Fort Collins, CO. (1971).

[6] C.R. Neil, A Reexamination of the Beginning of Movement for Coarse Granular bed Materials, Report IT 68, Hydraulic Research Station, Wallingford, England (1968).

[7] M.S. Yalin, and E. Karahan, Incipient of Sediment Transport, J. of Hyd. Division, ASCE 105: pp. 1433-1443 (1979).

[8] E.D. Andrews, Entrainment of Gravel From Naturally Sorted River Bed Material, Geological Society of America Bulletin, Vol. 94, pp. 1225-1531 (1983).

[9] C.H. Ling, Criteria for Incipient Motion of Spherical Sediment Particles, J. of Hydraulic Eng., Vol. 12 (16), pp. 472-478 (1995).

[10] S. Dey, and R. Raju, Incipient Motion of Gravel and Coal Beds, Sadhana Vol. 27, Part 5, pp. 559-568 (2002).

[11] J.C. Bathurst, Flow Resistance Estimation in Mountain Rivers, J. of Hyd. Engrg. ASCE, Vol. 111(4) pp. 625-643 (1985).

[12] R.H. French, Open Channel Hydraulics, McGraw-Hill Book Co., Singapore. ISBN 0-07-022134-0 (1986).

[13] W.H. Graf and M.S. Altinakar, Fluvial Hydraulics: Flow and Transport Process in Channels of Simple Geometry, Wiley, Chichester, England, ISBN 0-471-97714-4 (1998).

[14] C.E. Rice et al., Roughness of Loose Rock Riprap on Steep Slopes, J. of Hyd. Engeg., Vol. 124 (2), pp. 179-185 (1998).

[15] V.A. Vanoni, Sedimentation Engineering, ACSE Manual (54) (1975).

[16] P.L. Patel and K.G. Ranga Raju, Critical Tractive Stress of Non-Uniform Sediments, J. of Hyd. Res. 37: pp. 39-58, (1999).

[17] S. Dey, Sediment Threshold, Appl. Math. Modeling: 23, pp. 399-417 (1999).

Received August 20, 2003
Accepted August 31, 2005